



Article

Load Models Representative of Brazilian Actual Traffic in Girder-Type Short-Span Highway Bridges

Carlos Eduardo Rossigali ^{1,*} , Michèle Schubert Pfeil ² , Luis Volnei Sudati Sagrilo ²
and Hugo Medeiros de Oliveira ²

¹ Center for Marine Studies, Universidade Federal do Paraná, Beira-Mar Avenue, Pontal do Paraná 83255-976, PR, Brazil

² Civil Engineering Program, Universidade Federal do Rio de Janeiro, 149 Athos da Silveira Ramos Avenue, Rio de Janeiro 21941-972, RJ, Brazil

* Correspondence: carlos.rossigali@ufpr.br

Abstract: The Brazilian code NBR 7188 for highway bridge design prescribes a live load model consisting of a 3-axle vehicle plus a uniform load, which are both affected by an impact factor when considering dynamic effects. It does not play out actual traffic static effects and may be, in some cases, non-conservative. This work presents two load model configurations developed by gathering a real traffic database, traffic simulations, modeling of the dynamic interaction between vehicles and structure, and statistical extrapolations. Proposed load models comprise dynamic effects and were calibrated for two-lane single carriageway bridges with span lengths up to 40 m under free-flowing traffic. The target values of the effects were compared to those generated by the new proposed load models, as well as by the Brazilian design load model. Adequacy of the proposed models is demonstrated; results show that the effects generated by the Brazilian design load model are underestimated in many cases, particularly for negative moments in cantilevers.

Keywords: highway bridges; live load models; traffic simulation; vehicle-pavement-structure dynamic interaction; optimization



Citation: Rossigali, C.E.; Pfeil, M.S.; Sagrilo, L.V.S.; de Oliveira, H.M. Load Models Representative of Brazilian Actual Traffic in Girder-Type Short-Span Highway Bridges. *Appl. Sci.* **2023**, *13*, 1032. <https://doi.org/10.3390/app13021032>

Academic Editors: Tong Guo and Zhongxiang Liu

Received: 17 November 2022

Revised: 3 January 2023

Accepted: 5 January 2023

Published: 12 January 2023



Copyright: © 2023 by the authors. Licensee MDPI, Basel, Switzerland. This article is an open access article distributed under the terms and conditions of the Creative Commons Attribution (CC BY) license (<https://creativecommons.org/licenses/by/4.0/>).

1. Introduction

Codes for highway bridge design provide live load models for both ultimate limit states and fatigue evaluation. In the first case, the model intends to represent extreme traffic load effects, and in the second one, the magnitude of fatigue damage generated by the traffic or to ensure an unlimited fatigue life. Distinct techniques for traffic simulation as well as for the analysis and treatment of traffic data [1–9] have been developed, with the aim to assess bridge load effects by means of probabilistic methods and to improve the (re)calibration of live load models for design codes.

Eurocode 1 and AASHTO are reference design codes in relation to live load model development. Eurocode 1 [10] provides four models for vertical loads on highway bridges calibrated to represent the effects of the actual traffic, including dynamic effects [11]. Bridges spanning 5–200 m were chosen as representative structures. The basic model LM1 consists of three design lanes, each one loaded with a 2-axle vehicle and a uniformly distributed load. The original calibration of the Eurocode 1 load models was carried out using data from weigh-in-motion (WIM) traffic recorded between 1986 and 1987 [11,12]. A recalibration of the models was performed with new traffic data obtained from 1997 to 2001, which confirmed the values of the effects obtained in the original calibration [13].

On the other hand, the United States' design code AASHTO LRFD [14] provides two load models for actual traffic: the former AASHTO HL-93 design truck, for long spans, and a tandem axle for shorter spans. Both are accompanied by a 9.3 kN/m uniformly distributed design load. An impact factor is considered. Traffic simulation included the presence of multiple trucks on the slab, both in a single lane (convoys) and in adjacent

lanes (side-by-side and staggered), to determine the probability density functions (PDF) of the traffic effects on bridges [15]. Calibration of the models involved weighing 9250 heavy trucks in Ontario, Canada, in 1970s [12,16]. Approximately 200 bridges in the U.S. spanning 9–60 m were chosen as representative structures [17]. As a large amount of new WIM data has been collected within the U.S. over the past two decades [16], a recalibration has recently been performed. It was found that the current AASHTO load model is no longer suitable for short spans; therefore, Iatsko and Nowak [18] recommended increasing the tandem's load per axle from 110 kN to 130 kN.

In Hong Kong, WIM data from over 800,000 trucks were collected from five different locations; statistical analysis of traffic parameters was performed, such as GVW, axle weights, and wheelbases. Extreme daily bending moments and shear forces were calculated on simply supported bridges spanning 5–40 m. A 47-t 6-axle load model was obtained to represent the real traffic [19]. In Australia, load models have been developed considering the effects of traffic, future trends, and the presence of very long heavy trucks. The main ones are a “moving traffic load” and a “stationary traffic load”; both consist of four tridem groups plus a non-interrupted uniformly distributed load. The reference internal forces were shear and positive moments in simply supported bridges and negative moments in two-span continuous bridges spanning up to 100 m [20].

With the widespread use of WIM systems worldwide, the mentioned calibrations have already been carried out in several countries, e.g., South Africa [21] and Mexico [22].

To account for extreme load effects, the design code NBR 7188 [23] for highway bridges in Brazil presents a live load model, as shown in Figure 1, named TB-450, which is composed of a 450 kN weight vehicle and a distributed load p of 5.0 kN/m², both multiplied by an impact factor. This configuration originated from an older version of the design code. Load values have been increased over time as an attempt to update the code to account for heavy vehicles weights, although without any calibration process; therefore, loads from the Brazilian design code may not properly reproduce the extreme effects of the real traffic. There is a need to verify the adequacy of the code model and to develop more realistic design criteria.

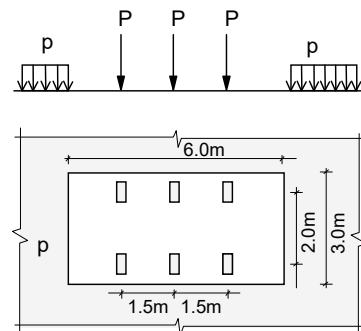


Figure 1. Current Brazilian load model: plan view and cross section.

Research focusing load models for highway bridge design is under development in Brazil [24–27]. The current fatigue live load model from the Brazilian code NBR 7188, which consists of the TB-450 model (see Figure 1) affected by a reduced factor, was evaluated to verify the unlimited fatigue life criterion of typical structures as box girders or multiple girders [28]. As a result, a new fatigue live load model was proposed.

Live load models for ultimate limit states in Brazilian highway bridges are being developed by the authors to reproduce extreme values of bridge effects due to actual traffic [6] (including dynamic effects) with approximately the same reliability index [17,29] among typical structural systems [13]. Two-girders reinforced concrete (RC) bridges, with span lengths up to 40 m, were considered. The adopted methodology, involving the developed traffic database, assessment of static and dynamic effects due to the real traffic, their histograms, and extrapolations, are described in Section 2.

Comparisons were provisionally made [30,31] between the values of the effects produced by the NBR 7188 load model and the characteristic values of the effects obtained by the simulations of actual traffic. Results showed that the Brazilian code load models could not adequately reproduce the real traffic of heavy vehicles and may, in many cases (particularly the negative moments at the cantilevers), be non-conservative. A similar situation also occurred in other countries [6,20–22].

Present work offers two main contributions to the research line. First, the grid models that represent the decks have undergone certain adjustments in order to simulate the static and dynamic behavior of the bridges in terms of displacements and natural frequencies. The new grid models were calibrated to shell element models of the bridges. Finally, two load models that are representative of Brazilian real traffic on small span bridges are proposed and comparisons between their results and those of the NBR 7188 current model are presented.

2. Methodology

The adopted methodology consisted of the following steps [11,13,17,30]:

- (a) Traffic database: from traffic data obtained by static scales and WIM equipment on highways, a comprehensive database was built and the necessary statistical information about traffic was obtained;
- (b) Selection of typical structural schemes and critical internal forces;
- (c) Static effects due to the real traffic: were assessed by determining critical internal forces in structural models of the selected typical bridges;
- (d) Dynamic effects: considered through analyses of the vehicle-pavement-structure interaction;
- (e) Target values of the effects due to real traffic: histograms of the static effects were obtained, to which PDFs were fitted and extrapolations were made to certain return periods. The characteristic internal forces were then affected by dynamic amplification factors leading to the target values;
- (f) Load models representative of the actual traffic: features of new load models were sought by optimization in order to approximately reproduce the extreme values of the critical effects (the target values), including the dynamic contribution, with the design load statically applied to the corresponding structural models.

3. Traffic Database







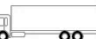


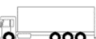






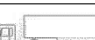






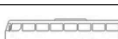

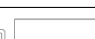

The first stage was the elaboration of a representative real traffic database gathering information on sources like weighing at monitoring stations, traffic surveys, and traffic parameters measurements in free flow, that were carried out at different locations in Brazil [24].

Data collected during 14 consecutive days in 2011 at a weighing station on SP-348 state highway is fairly representative of the heavy traffic in Brazil, so it was taken as reference to the database developed in this work [30]. As the available data did not include information on buses, vehicle speed, and wheelbases, additional information was gathered from other four data sources including weighing stations and traffic surveys: (a) a traffic survey in 15 stations in several States of Brazil between 1999 and 2002 by means of WIM measurements; (b) a traffic survey on federal Brazilian highways by collecting data in 109 counting stations spread all over the country in a 7-day period in 2005; (c) data collected at the same weighing station in SP-348 state highway consisting of a set of sheets containing daily records of a 6-day period in June 2008; (d) data from a weighing station located on BR-277 federal highway, containing daily records of a 28-day period in June 2008. It was found that the statistical information of all these data is quite similar, and that the adoption of a hybrid base would not yield important deviations. Also, more recent traffic surveys [32] indicate very similar patterns in Brazilian traffic today, in relation to the older data used in this work. However, GVW distributions for the Brazilian case are not similar to those obtained from Eurocode 1 and AASHTO LRFD calibration [11,12,15,18]. This was

expected, as regulations for truck classes, weights, wheelbases, and lengths differ from country to country.

The database consists of the configurations of commercial vehicles illustrated in Table 1 together with their frequency. Classes 2S3 and 3S3 were divided into subclasses short (S) and long (L). Light vehicles, such as cars, pick-ups, vans, motorcycles, and tricycles, were discarded since they are not relevant to traffic simulation in short-span bridges [1].

Table 1. Spectrum of Brazilian commercial vehicles: class, silhouette, and relative frequency.

Class	Silhouette	%	Class	Silhouette	%	Class	Silhouette	%
2CC		11.07	2S1		4.48	3I1		0.21
2C		12.42	2S2		11.97	3I2		0.13
3C		17.11	2S3		11.36	3I3		1.59
4C		0.15	2I1		0.15	3T4		4.64
2C2		1.50	2I2		1.78	3T6		0.85
2C3		0.28	2I3		0.37	3M6		0.17
3C2		0.28	3S1		0.17	2CB		7.95
3C3		0.25	3S2		0.74	3CB		2.04
3D4		0.16	3S3		6.15	3BB		2.04

To perform the traffic simulation, PDFs were fitted to each one of the vehicle classes GVW histogram [13]; the best model was chosen among most usual continuous functions. After testing these models individually or with particular linear combinations of them (depending on the number of modes of each histogram), the most appropriate model was elected via goodness-of-fit tests. The method of moments was used to perform the parameters' estimation. Axle weights were also considered as random variables. To avoid the use of correlations between axle weights, the scatter diagrams relating the axle groups weights to the GVW, for each vehicle class, were submitted to adjustment curves by means of linear regression [33]. Most wheelbases were considered random variables, which were fitted to PDF models as performed for the GVWs [8]. Tandem and tridem wheelbases and other distributions with small coefficients of variation were considered deterministic. More details can be found in [30].

4. Structural Models

In this work, RC bridges (molded in situ), with a Π cross-section—slab and two girders—, were considered (see Figure 2a). Three longitudinal structural schemes were analyzed: simply supported, two-span continuous, and cantilever, the latter representing the existing cantilever ends of the supported or continuous bridges. The adopted span lengths L are 10 m, 20 m, 30 m, and 40 m for simply supported and continuous bridges, and 2.5 m, 5.0 m, 7.5 m, and 10 m for cantilevers, as shown in Figure 2b. The internal forces and sections used as reference are [8,13,15]:

- Shear force at the support of simply supported systems and at the central support of two-span continuous systems;
- Positive moment at the midspan of simply supported systems and near to the midspan of two-span continuous systems;
- Negative moment at the support of cantilever systems and at the central support of continuous systems.

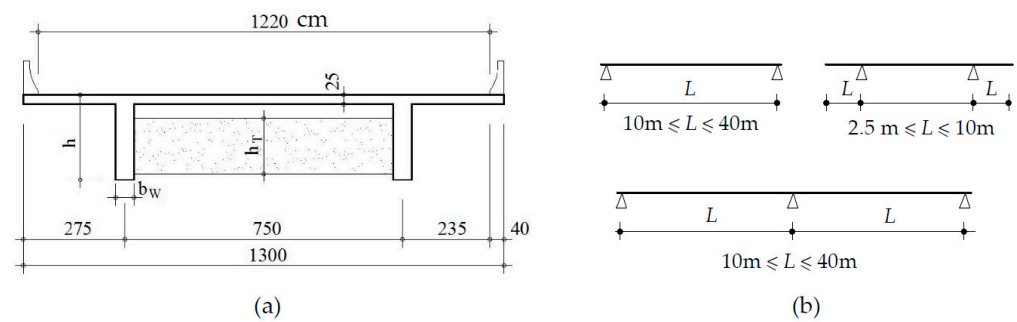


Figure 2. (a) RC II cross section adopted (units: cm) and (b) structural schemes.

Total bridge width equal to 13 m, as shown in Figure 2a, corresponds to the Brazilian standard deck for single carriageway two-lane highways. It supports roads with two traffic lanes, 7.20 m wide. This set of geometry and structural systems is quite representative of the general pattern of Brazilian highway bridges [25].

Table 2 presents the dimensions adopted for the structural elements illustrated in Figure 2a. The usual design pattern for reinforced concrete bridges is adopted. Cross beams have rectangular cross-sections and are considered disconnected to the slab. In addition to the support cross beams, two intermediate cross beams were considered for the 10 m and 20 m spans and three for the 30 m and 40 m spans. For the cantilevers, one intermediate cross beam was considered for the spans of 2.5, 5.0, and 7.5 m and two for the span of 10 m. The concrete compressive strength f_{ck} was assumed equal to 25 MPa for all bridges.

Table 2. Dimensions of the structural elements.

Element	Dimension	Simply Supported Span Lengths (m)				Cantilever Span Lengths (m)			Continuous Span Lengths (m)				
		10	20	30	40	2.5	5.0	7.5	10	10	20	30	40
Girder	h	1.00	2.00	3.00	3.50	0.90	1.80	2.50	3.00	0.90	1.80	2.50	3.00
	b_w	0.35	0.40	0.45	0.50	0.35	0.40	0.45	0.50	0.35	0.40	0.45	0.50
Cross beam	h_T	0.80	1.60	2.40	2.80	0.70	1.40	2.00	2.40	0.70	1.40	2.00	2.40
	b_T	0.30	0.35	0.40	0.45	0.30	0.35	0.40	0.45	0.30	0.35	0.40	0.45

The identification pattern of the structures consists of a letter that represents the structural scheme [S: simply supported; C: continuous; F: fixed (clamped-free)], followed by a number that indicates the span length (in meters). For the analyzed bridges, 3D shell models were created, as shown in Figure 3a.

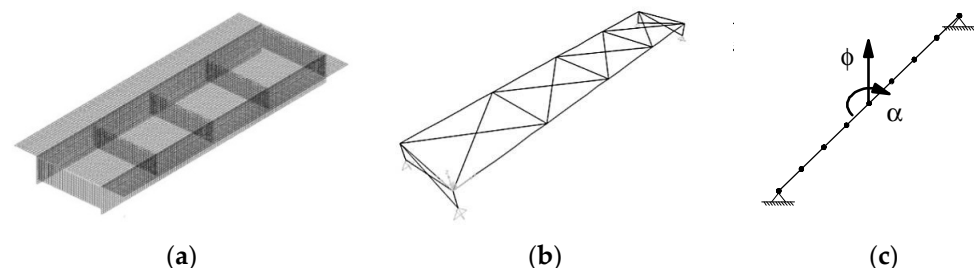


Figure 3. (a) Finite element model for the 30-m span simply supported bridge (S-30). (b) Equivalent grid model. (c) Stick model for dynamic analyses.

In order to reduce the computational effort required for several structural analyses of the traffic simulation, an equivalent grid structural model, shown in Figure 3b, was developed to represent the finite element model of Figure 3a. The adjusted grid model was then used for static analysis of traffic simulations and also to create the equivalent

stick model shown in Figure 3c, which represents the bridge in the analyses of the vehicle-pavement-structure dynamic interaction (Section 6).

For each bridge structure, a Finite Element Model (FEM) was developed with four node quadrilateral shell elements whose formulation is based on Mindlin/Reissner theory, which accounts for shear behavior, to represent girders, slab, and crossbeams (Figure 3a).

In the grid model the girders and cross beams are modeled with spatial frame elements. The geometric properties of the girders are calculated for a T cross-section, considering the portion of the slab that contributes to the stiffness. The effective width of the flange is defined by geometric conditions and the rules given by the Brazilian standard for design of concrete structures [34]. Girders and cross beams have a constant cross-section.

Diagonal and vertical elements were modeled with a polygonal section and dimensions defined by the adjustment to the shell model. Diagonal elements arranged in “X” in the grid plane were created to simulate the deck slab; vertical and diagonal elements forming a “X” on the planes of the end cross beams were created to simulate the eccentricity of the girders’ supports in relation to their center of mass.

The adopted modeling procedures and the technique by which a 3D-grid model as the one described above is developed in adjustment to a 3D numerical model composed of shell elements were validated by comparison to experimental results in Santos et al. [35].

Given the transverse configuration of the bridge (II cross-section) and the presence of cross beams, an analytical solution for the transverse load distribution from the Courbon–Engesser method could be considered, as recently applied in [36], since its fundamental hypotheses are expected to be valid. In fact, comparisons between analytical and numerical (grid model) load factor distribution showed a maximum difference of only 5.2% for load eccentricities on the unfavorable side for the considered girder. However, the analytical solution for the longitudinal structural scheme considering a simple beam does not provide a faithful representation of the bridge stiffness. This way, the described numerical models were applied for static and dynamic analyses.

Table 3 presents the comparison between results from the detailed shell model—Figure 3a—and the equivalent grid model—Figure 3b—in terms of dead loads of the structures, midspan displacements due to the passage of a class 3C truck (Figure 4) along the center line of the bridge, and the right girder (G1), as well as the natural frequencies in vertical bending and longitudinal torsion modes of simply supported bridges (S). Comparative results show that the grid model was successfully calibrated to the shell model.

Table 3. Maximum deflections and natural frequencies from the grid model and shell model for simply supported bridges (B = bending; T = torsion).

Bridge	Model	Deflections (m) Due to a 3C Truck at Transverse Positions		Natural Frequencies (Hz)	
		Center Line	Above Girder G1	1st B	1st T
S-10	Shell	6.10×10^{-4}	2.95×10^{-4}	11.63	14.21
	Grid	6.58×10^{-4}	2.98×10^{-4}	14.37	15.13
S-20	Shell	4.14×10^{-4}	8.08×10^{-4}	7.76	7.25
	Grid	4.13×10^{-4}	9.10×10^{-4}	8.67	9.55
S-30	Shell	4.77×10^{-4}	9.11×10^{-4}	6.40	7.22
	Grid	4.74×10^{-4}	9.01×10^{-4}	6.71	7.87
S-40	Shell	6.72×10^{-4}	12.5×10^{-4}	4.56	6.21
	Grid	6.77×10^{-4}	12.3×10^{-4}	4.67	5.65



Figure 4. Passage of the three-axle rigid vehicle [3C]. (a) Along the center line of the bridge. (b) Over the right girder (G1).

Values of deflections and natural frequencies for each bridge span depend on the adopted dimensions for the structural elements (see Table 2). It can be seen in Table 3 that vertical deflections increase with span length for loads above girder G1. As expected, natural frequencies associated to vertical bending and torsional modes decrease with the increase of the span length.

5. Traffic Simulation for Static Analysis

5.1. Traffic Simulator and Structural Analysis

The computational tool developed to obtain the effects generated by real traffic consists of two steps [2]:

- Traffic simulation: initial stage in which information is generated for all vehicles that will make up the traffic, such as vehicle classes, speeds, etc. For the variables described by PDFs, the Monte Carlo technique is used to generate values [1,4,6,7,9,37].
- Structural analysis in time: stage in which the vehicles generated by the simulation travel along the analyzed structure, loading it. The effects due to each load are calculated by means of influence surfaces for unitary concentrated force, bending, and torsion moments at the critical sections; these effects are recorded at each instant of time and the maximum values in each loading cycle of the structure are saved. At the end of the process, these maximum values are summarized in histograms.

A queue of vehicles is generated at each lane, as well as the values of some variables (random or deterministic) of the vehicles that will travel on it. Traffic is generated in each lane separately and independently. The class is the first variable to be generated for each vehicle in the queue, also using the Monte Carlo technique, depending on the probability of occurrence of each class (Table 1). Once the class is defined, all other information relevant to this vehicle is generated: wheelbases, speed, time until the next vehicle, and GVW. Defined the gross weight, the static load of each axle or group of axles is then calculated (instead of estimated) by means of regression lines.

The traffic simulator checks whether, at the current instant of time, there is any vehicle with at least one axle on the bridge. If so, the desired effects are calculated, neglecting the initial deformations of the structure at each time. The structural analysis ends only when all vehicles on all lanes have already traveled over the bridge; when this happens, all the values of the effects obtained are organized in histograms.

According to O'Connor and O'Brien [3], some different traffic situations should be considered: traffic jams, mixed flow, and free flow. In small spans, critical load cases are due to heavy vehicles crossing and are affected by the dynamic amplification factor [3,4,29]. In large spans, however, critical load cases are due to the simultaneous presence of several vehicles on structures in congested or mixed flow, with little or no dynamic amplification [13]. As the structures considered herein have a maximum length of 40 m, congested and mixed flow situations were not considered: simulation was performed only in the free flow modality.

For the traffic analysis, eight different scenarios were defined (Figure 5), varying the position and direction of the lanes and the transverse position of the vehicles, aiming to map a large amount of possibilities for vehicle arrangements among the lanes [38], and in addition, to forecast possible exceptional situations such as vehicles traveling close to the

Jersey barrier, which are needed for the Ultimate Limit State design. The vehicles' positions always simulate the worst situation for the right girder (G1). In even-numbered scenarios, there is a reallocation of lanes to characterize exceptional or emergency situations [11].

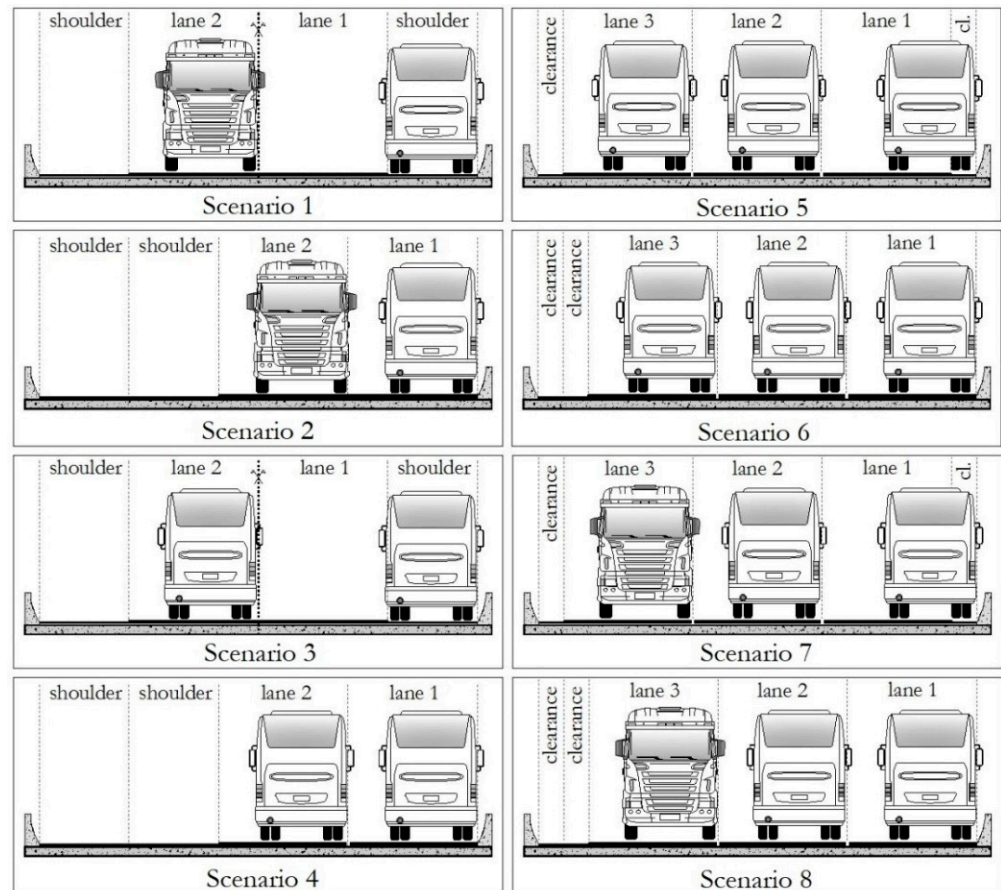


Figure 5. Traffic scenarios considered for the Ultimate Limit State design [30].

5.2. Considerations for Traffic Simulations

Assuming the bridge loading process as stationary, traffic simulations were carried out for 30 consecutive days. This period of simulation is sufficient to ensure an accurate generation of the characteristic values of effects [3,24] and avoid large computational effort from long-run simulations [6,38].

The subsequent step is the extrapolation of the distributions of the effects to certain return periods. For Eurocode 1 load models calibration, the target values were taken with a return period of 1000 years to ensure a small probability of excess in the effects' values: 0.1% per year [11]. This choice was made to limit the likelihood of several exceedances of the serviceability limit state during the lifetime. The AASHTO load model HS93 was calibrated assuming a return period of 75 years [15]. To set the return period for the extrapolations of static effects, one should consider that a very large return period is not representative, because the traffic probably will not remain with the same settings. The rapidly changing technology causes distortion of the load pattern in long-term violating the stationarity of these random processes, which partially invalidates the large return periods, unlike natural phenomena. On the other hand, the extrapolation is being held for random unmeasured but indirectly modeled quantities—the internal forces—which can generate errors, so that for safety, conservatively large return periods must be adopted [13]. Considering both aspects, it was assumed 100 years for simulations in Scenarios 1, 3, 5, and 7, and 10 years for Scenarios 2, 4, 6, and 8 [39]. In all cases, traffic growth was not considered for extrapolation. Speeds lower than 30 km/h or greater than 140 km/h were also not considered.

Available data referring to the current speed of the vehicles (measured in the traffic lanes) were obtained only in the form of histograms; the records containing the time between subsequent vehicles were not available, so that it was not possible to fit a PDF to this variable. Therefore, due to the lack of this specific type of discriminated records, time between vehicles was modeled by a gamma distribution [3,33] with a coefficient of variation assumed equal to 0.5. The adoption of this distribution is suggested in the case of the process of vehicles arrival to be idealized as a Poisson process [7]. The Average Daily Truck Traffic (ADTT) for the adopted database is 7019 commercial vehicles. This value is called the reference flow (RF) and includes traffic on three lanes.

At this stage of the work, the several correlations due to the interdependence among GVWs, speeds, headways, and wheelbases, in the same lane and in adjacent lanes, were not considered for the traffic simulations. On the one hand, they are relevant in multi-lane, same-direction traffic (Scenarios 4 to 8 in Figure 5) on short-to-medium span bridges due to the dependence between lanes [1] and may increase the maximum effects [40]. On the other hand, in [24], it was found that the statistical parameters of the distributions of effects generated when considering small negative correlations between GVWs and speeds, in the same traffic lane, are identical to those generated with zero correlation; furthermore, Anitori et al. [5] found no correlation between the GVWs of vehicles close to each other, neither in the same lane nor in adjacent lanes.

If there is an equal number of lanes for each traffic direction, it can be roughly considered that total highway traffic is divided equally for each direction; however, partition of the flow in each direction between lanes, when there is more than one lane, is not uniform: the right lane tends to receive most of the commercial vehicle traffic, as slower vehicles are advised to travel in this lane. The proportions shown in Table 4 were adopted for the division of the flow [13,37,40].

Table 4. Characterization of traffic scenarios (RF = reference flow = 7019 vehicles per day).

Scenario	Lane 1		Lane 2		Lane 3	
	Dir.	%RF	Dir.	%RF	Dir.	%RF
1 and 2	Go	85%	Return	85%	-	-
3 and 4	Go	85%	Go	15%	-	-
5 and 6	Go	80%	Go	18%	Go	2%
7 and 8	Go	85%	Go	15%	Return	85%

Table 5 shows the maximum effects obtained in the reference sections and the trucks and buses that have originated them. In some cases, there was a simultaneous presence on the bridges of two very heavy vehicles, although GVW values never came very close to their physically accepted limits [24]. Thus, it is understood that the several cases of the simultaneous presence of vehicles in different lanes of the carriageway analyzed in the literature [3,32,41], are automatically included by the random character of the variables that define the traffic simulation, except the free flow of truck convoys on the same lane. On lane 1 (which has the greatest influence surface ordinates of each effect), in extreme cases, the shortest bridges are loaded mainly by the heaviest tridem axles of the most frequent semi-trailers (2S3 and 3S3), while on longer bridges, the presence of the longest 3T4 and 3T6 heavy vehicles prevails, because they can fit entirely into these structures.

Table 5. Vehicle configurations that generated the extreme static effects on the bridges.

Bridge	Effect	Value (kN/ kNm)	Scenario	Vehicle n° 1				Vehicle n° 2				Vehicle n° 3			
				Lane	Class	GVW (kN)	Speed (km/h)	Lane	Class	GVW (kN)	Speed (km/h)	Lane	Class	GVW (kN)	Speed (km/h)
S-10	M+	587.4	3	1	2S3-L	616.9	80	2	3C	229.7	80	-	-	-	-
	V	514.5	3	1	2S3-S	693.9	80	2	2S3-L	411.6	80	-	-	-	-
S-20	M+	2100.2	1	1	2S3-L	554.0	80	2	3S3-L	632.6	60	-	-	-	-
	V	693.7	8	1	3T4	530.4	80	2	2S3-L	625.2	80	-	-	-	-
S-30	M+ V	4927.7	8	1	3T4	727.5	100	2	3I3	541.1	80	-	-	-	-
S-40	M+	6981.6	5	1	3S3-L	699.8	80	2	3S3-L	511.2	80	3	3C	144.3	60
	V	882.0	8	1	3T4	638.1	100	2	2S3-L	575.9	60	3	2C	83.4	100
C-10	M+	569.6	5	1	3S3-L	798.0	80	2	2S3-L	299.5	80	3	2CB	121.2	60
	V	531.1	5	1	3S3-L	798.0	80	2	2S3-L	299.5	80	3	2CB	121.2	60
	M ⁻	848.5	8	1	3S3-L	689.3	100	2	3S3-S	471.2	80	-	-	-	-
C-20	M+	2051.7	6	1	2S3-S	596.2	100	2	3C	236.9	80	3	3T6	620.3	100
	V	724.8	7	1	3T4	719.1	100	2	3S3-L	528.1	60	-	-	-	-
	M ⁻	1932.5	6	1	3T6	798.5	80	2	3T6	783.5	60	-	-	-	-
C-30	M+	3922.2	5	1	3T6	751.7	80	2	3S3-L	669.8	80	-	-	-	-
	V	856.1	8	1	3T4	726.3	80	2	3T6	741.5	80	-	-	-	-
	M ⁻	3208.8	4	1	3S3-L	464.8	80	1	3T6	686.9	80	2	2I3	426.7	80
C-40	M+	6062.4	7	1	3T4	808.4	80	2	2S3-S	436.1	60	-	-	-	-
	V	934.2	7	1	3T4	704.5	60	2	3T6	705.7	80	-	-	-	-
	M ⁻	4710.6	3	1	3T6	838.2	80	1	3T4	573.7	60	-	-	-	-
F-2.5	M ⁻	595.9	8	1	3S3-L	881.4	80	-	-	-	-	-	-	-	-
F-5.0	M ⁻	1745.0	4	1	3S3-L	806.9	80	2	2S3-S	710.7	80	-	-	-	-
F-7.5	M ⁻	2473.6	5	1	2S3-L	483.4	80	2	2S3-L	473.2	80	-	-	-	-
F-10	M ⁻	3350.0	8	1	3S3-L	697.0	80	2	2S3-S	440.3	80	3	3I3	449.8	80

6. Analysis of the Vehicle-Pavement-Structure Interaction

The first analytical models to address bridge dynamic behavior under traffic load consisted of beams subjected to moving loads [42]. Regarding the problem of the vehicle-bridge dynamic interaction considering the pavement roughness, the motion equations of the structure are derived and coupled to the vehicle motion equations ensuring equilibrium and displacement compatibility at the contact points [43]. The bridge may be represented as a simple beam in vertical bending; a 3D beam, including torsional vibration modes; a grillage system [44]; or by finite element discretization [45]. In general, vehicle models consist of mass-spring damper multi-degree of freedom systems, which are either plane or 3D [44,45]. A simplified model represents the vehicle as a moving load plus a pre-defined forcing function as usually done in the footbridge—pedestrian interaction problem [46].

In this work, an analytical-numerical model was developed and implemented aiming to perform the analysis of the vehicle-pavement-structure dynamic interaction. A three-axle vehicle is considered to be moving at a constant velocity along the bridge with eccentricity relative to the bridge axis. The vehicle is represented by a plane system of rigid bodies—see Figure 6a—connected by springs (k_{vi} and k_{pi}) and dampers (c_{vi} and c_{pi}), and is associated to five degrees of freedom: vertical displacement (u_v) and rotation (θ_v) of the suspended mass (m_v) and vertical displacements (u_{pi}) of the three non-suspended masses (m_{pi}). The bridge structure motion is considered by generalized coordinates (u_e) in terms of vertical bending and torsion vibration modes and corresponding frequencies associated to the stick model of Figure 3c. These dynamic characteristics of the bridge are identified using the equivalent grid model shown in Figure 3b. Displacements and internal forces are calculated by the modal superposition method. From the analytical models of vehicle and structure, the

coupled system equations are formulated, including the presence of the rough pavement. The motion equation associated to the structure j^{th} vibration mode is written as:

$$m_{ej}\ddot{u}_{ej} + c_{ej}\dot{u}_{ej} + k_{ej}u_{ej} = \sum_{i=1}^3 \varphi_{jk}F_{ei}, \tag{1}$$

where m_e , c_e and k_e correspond to the generalized mass, damping, and stiffness parameters and φ_{jk} is the j^{th} eigenvector component at node k of the structure where there is a tire contact point. At each vehicle-structure contact point, interaction forces of elastic (f_{ei}) and damping (f_{di}) components are generated as functions of the relative displacement and velocity between the axle mass m_{pi} and the structure contact point, considering the pavement roughness profile (u_r), as shown in Figure 6b.

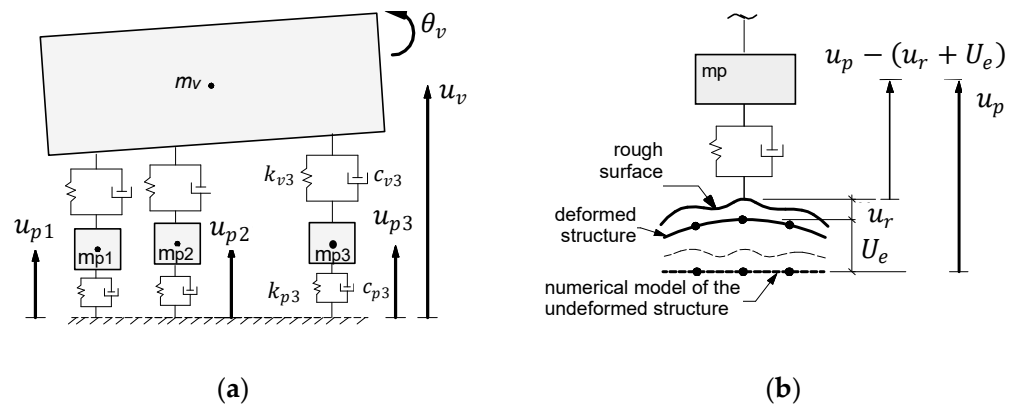


Figure 6. (a) Analytical model of the rigid three-axle vehicle (class 3C). (b) Axle-structure contact point displacements.

For the i^{th} axle, located at node k where the vertical displacement is equal to U_{ek} , the interaction force is written as:

$$F_{ei} = f_{ei} + f_{di} \tag{2}$$

where

$$f_{ei} = k_{pi} [u_{pi} - (U_{ek} + u_{rk})] \tag{3}$$

$$f_{di} = c_{pi} [\dot{u}_{pi} - (\dot{U}_{ek} + \dot{u}_{rk})] \tag{4}$$

The pavement surface roughness function was obtained by random generation from a power spectrum [47]. To represent discontinuities in surface resulting, for instance, from lack of proper maintenance of expansion joints or soil settlement under a transition slab, a 3-cm step at the bridge entrance was also considered in addition to the pavement roughness. Time integration of the resultant motion equations is performed by the Runge–Kutta method. Analysis of the vehicle-pavement-structure dynamic interaction leads to the Dynamic Amplification Factor (DAF), defined by the ratio between the maximum dynamic and the static effects:

$$DAF = E_{dyn}/E_{st} \tag{5}$$

7. Target Values of the Effects Due to Real Traffic

The steps adopted to obtain the target values of the effects due to real traffic, in the case of free flow, are the following:

- (a) Fit Weibull PDFs to the tail of the histogram of each static effect [2,4,6,8,9,16,21], for all scenarios in Figure 5, and extrapolate to the corresponding return periods, obtaining their representative values. The Weibull PDF is one of the most widespread distributions in the literature for modeling extreme value events. As well as in other PDFs adopted for traffic simulation, the parameters of these distributions were

- estimated by the method of moments. The largest extrapolated value among all scenarios is considered as the characteristic static value of each effect [24].
- (b) Perform the dynamic analysis of the whole loading that have caused the characteristic static effect in the reference traffic scenario (Table 5), in order to obtain the DAF for this configuration. This dynamic amplification is taken conservatively as representative of the effect on the structure. The reason for that lies in the fact that, although dynamic amplifications are greater for lighter vehicles [13,48,49], dynamic effect always increases with static effect [50,51].
 - (c) Obtain the target values of each effect in each structure, to be reproduced by the load model, by multiplying the characteristic static value of the static effect by the corresponding DAF.

To apply step (b) consistently, for each analyzed effect on each bridge, all vehicles that generated, together, the maximum static effect should be considered in the dynamic analysis. However, up to now, it has been carried out by a simplified procedure, since the analytical-numerical model for the dynamic analysis (Section 6) has been validated experimentally only for class 3C vehicles [25]. Aiming to apply this model for other vehicle configurations, the concept of an equivalent 3C vehicle was devised in which vehicles of other classes are reduced to a 3C truck [27]. Figure 7 shows examples of this reduction. Each axle of the 3C truck may represent a group of axles of the actual vehicle with equivalent properties of mass, stiffness, and damping of the original ones, so that natural frequencies of the fundamental vibration modes of both mechanical systems are similar.

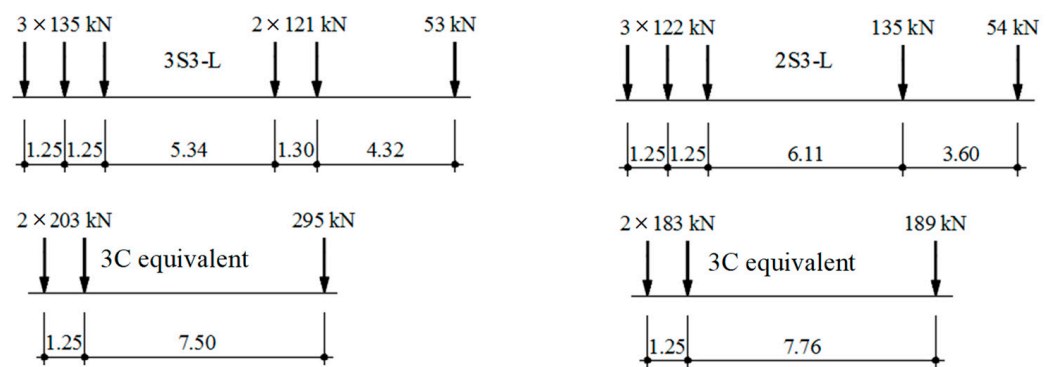


Figure 7. Some 3C-equivalent trucks. Units: m.

For the sake of simplification, only a single equivalent vehicle was used and standardized for each class of original vehicle, regardless of their wheelbases and GVW; for this, the values of these two quantities were averaged among all vehicles of each class that generated the greatest static effects (Table 5); the results are shown in Table 6. In the case of simultaneous presence of vehicles on the bridge when the maximum static effect occurs, only the vehicle that generated the most unfavorable effect was considered. In each structure, for each reference effect, the dynamic amplifications are obtained for 2S3-S, 2S3-L, 3S3-L, 3T4, and 3T6 trucks, each of them traveling alone, with speeds ranging from 20 km/h to 100 km/h. For each case, the DAF is taken as the highest value obtained in each analysis. Then, the maximum DAF value is retained for each pair structure-vehicle, regardless of the reference effect considered. Table 7 shows the statistical features of static effects' distribution, obtained by fitting Weibull distributions to the corresponding histograms, as well as the dynamic amplifications and the target values of the effects.

Table 6. GVWs and wheelbases of standardized 3C equivalent vehicles for each truck class.

Original Vehicle	d ₁₂ (m)	d ₂₃ (m)	P ₁ (kN)	P ₂ (kN)	P ₃ (kN)
2S3-S	4.63	1.25	217.85	213.61	213.61
2S3-L	8.11	1.25	188.33	181.54	181.54
3S3-L	7.96	1.25	298.72	213.64	213.64
3T4	7.30	4.74	268.75	206.82	217.90
3T6	11.06	8.84	238.17	367.36	190.59

Table 7. GVWs and wheelbases of standardized 3C equivalent vehicles for each truck class.

Bridge	Effect	Parent 'Static' Distribution (kN/kNm)			Maximum DAF for Several Velocities					Dynamic (Target) Value (kN/kNm)
		\bar{X}	s	Charact. value	2S3-S	2S3-L	3S3-L	3T4	3T6	
S-10	V	325.9	24.8	715.0	1.33	1.28	1.30	-	-	950.2
	M+	383.8	29.7	750.5						997.4
S-20	V	438.2	37.5	879.3	1.09	1.15	1.12	1.14	1.17	1027
	M+	1291	81.0	2711						3167
S-30	V	548.6	44.5	1059	1.09	1.13	1.08	1.10	1.14	1206
	M+	3310	270.3	5789						6595
S-40	V	555.5	49.4	1113	1.13	1.13	1.13	1.10	1.18	1309
	M+	4601	358.3	9326						10,964
C-10	M+	328.8	24.9	641.6	1.32	1.20	1.20	-	-	846.7
	V	326.5	23.0	613.2						809.1
	M ⁻	498.9	41.5	1045						1378
C-20	M+	1222	108.1	2446	1.08	1.15	1.12	1.19	1.25	3050
	V	435.5	34.6	909.7						1135
	M ⁻	1222	106.5	2737						3414
C-30	M+	2524	205.6	4883	1.11	1.17	1.10	1.12	1.16	5699
	V	552.9	49.0	1058						1235
	M ⁻	2185	162.5	4266						4978
C-40	M+	3840	321.7	7798	1.21	1.16	1.15	1.14	1.21	9437
	V	553.7	46.3	1160						1404
	M ⁻	3226	218.8	6334						7665
F-2.5	M ⁻	385.6	30.7	762.3	1.67	1.49	1.60	-	-	1275
F-5.0	M ⁻	1098	88.6	2226	1.29	1.36	1.51	-	-	3357
F-7.5	M ⁻	1641	124.9	3201	1.33	1.48	1.49	-	-	4768
F-10	M ⁻	2223	195.2	4475	1.38	1.31	1.18	-	-	6159

8. Load Models Representative of the Actual Traffic

Once the target values of the effects are defined, the physical and geometric configurations of load models that adequately represent the real traffic were sought by optimization via exhaustion, so that, with the loading of these fictitious models statically applied to the structures considered, they reproduce approximately the target values at the critical cross-sections of each one, automatically including the dynamic amplification. Defining geometric features such as number of axles, wheelbases, transverse distances between tires, number and width of the design lanes, and considering the values of concentrated and uniformly distributed loads as optimization parameters, a scan is performed in all possible combinations inside the domain of each variable, discretizing the total weight of the design vehicle (concentrated forces) in multiples of 50 kN and the distributed in

multiples of 0.5 kN/m². Geometric information about the bridges' superstructure and the target values (Table 7) are also provided.

The load models sought consisted of a vehicle composed of some concentrated forces, as well as distributed loads. The variable loads do not act in a favorable fashion; therefore, forces distributed by area only act in the regions of the deck that generate adverse effects to the analyzed element (in this case, the right girder). If there is more than one design lane, the effective width of the deck (region where the influencing surfaces only generate unfavorable effects) is divided so that the first lane is located at the most severe transversal position for the structural element considered. The remaining area of the deck is considered for the remaining width—vehicles do not load it.

For the deck type shown in Figure 2a, a weight factor (W_{ij}) is defined according to the structural system and the internal force [24]:

$$W_{ij} = W_j^{struct} \cdot W_{ij}^{effect} \quad (6)$$

Sub-indexes i and j refer, respectively, to internal forces and structures. Values adopted for W_j^{struct} were 2.0 for simply supported and continuous systems and 1.5 for cantilevers. For W_{ij}^{effect} , 2.0 for moments and 1.5 for shear forces were adopted.

The objective function is the weighted error: the sum of all relative differences between each effect generated by the candidate load model, and the corresponding target value. According to Table 7, to compose the objective function, there are 24 effects in 12 structures. Steps for seek are defined as follows [11]:

- calculate each internal force i generated in each structure j by the load model k (E_{ijk});
- calculate the relative difference (ε_{ijk}) between E_{ijk} and the corresponding target value of the effect (T_{ij}):

$$\varepsilon_{ijk} = \left| \frac{E_{ijk} - T_{ij}}{T_{ij}} \right| \quad (7)$$

- calculate the weighted error for load model k :

$$\bar{\varepsilon}_k = \frac{\sum_i \sum_j W_{ij} \varepsilon_{ijk}}{\sum_i \sum_j W_{ij}} \quad (8)$$

For each set of geometric features, the load model with the smallest weighted error (m^{th} , $1 \leq m \leq \text{NLM}$) is chosen as the most appropriate (NLM: number of load models). Several hypotheses were tested; each one considered a different set of geometric characteristics and search restrictions in the relative and absolute values of the loads per design range. The width of the design lane was set at 2.00 m. Some possibilities were considered: one or three design lanes; design vehicle with two or three axles; and wheelbases measuring 1.30 m or 1.50 m. The seek process was carried out by choosing two load models considered as representative of the actual Brazilian traffic in these structures (Figure 8), named "load model 1" and "load model 2". Interruption of the load distributed around the design vehicle contour, as done in NBR 7188, was not considered. In both models, the wheelbase was equal to 1.50 m, similar to the model from the Brazilian design code. Weighted errors for models 1 and 2—Equation (8)—are 6.9% and 5.6%, respectively. The load model 2 follows the configuration of the Eurocode 1 model LM1. One of the AASHTO live load models also consists of a design tandem as in load model 1, but is combined to a linear distributed load.

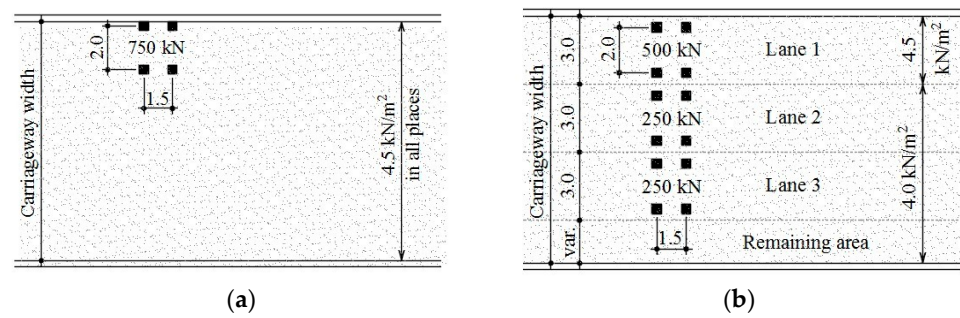


Figure 8. Plan view of the proposed load models: (a) load model 1; (b) load model 2. Units: m.

Load model 1 consists of a distributed load of 4.5 kN/m² over the entire effective width of the decks, as well as a 750 kN two-axle vehicle. Load model 2 comprises three two-axle vehicles, weighing 500 kN in lane 1 and 250 kN in lanes 2 and 3, as well as distributed loads of 4.5 kN/m² in lane 1 and 4.0 kN/m² in other (effective) deck places.

9. Comparison between Target Values and the Effects Generated by Load Models

In Figures 9–11 the target values are compared to the effects generated by load models 1 and 2; the NBR 7188 TB-450 model [23] is also used for comparisons, including its impact factor. Ratios between effects generated by each load model and the corresponding target values are shown in Table 8.

Table 8. Ratios between the effects generated by each load model and the corresponding target values.

Bridge	Effect	Load Model		NBR 7188
		1	2	
S-10	V	0.88	0.87	0.70
	M+	1.08	1.04	0.79
S-20	V	0.96	0.95	0.83
	M+	1.09	1.06	0.91
S-30	V	0.94	0.93	0.87
	M+	1.14	1.08	0.95
S-40	V	0.97	0.95	0.93
	M+	1.04	0.99	0.90
C-10	M+	1.10	1.06	0.80
	V	1.08	1.05	0.87
	M ⁻	0.91	0.87	0.66
C-20	M+	1.04	1.00	0.87
	V	0.93	0.91	0.86
	M ⁻	0.82	0.85	0.85
C-30	M+	1.09	1.04	0.93
	V	1.01	0.99	1.03
	M ⁻	0.96	1.05	1.12
C-40	M+	1.01	0.97	0.89
	V	1.01	0.99	1.01
	M ⁻	0.94	1.07	1.19
F-2.5	M ⁻	0.98	0.96	0.50
F-5.0	M ⁻	0.92	0.93	0.58
F-7.5	M ⁻	0.94	1.00	0.66
F-10	M ⁻	0.94	1.04	0.70

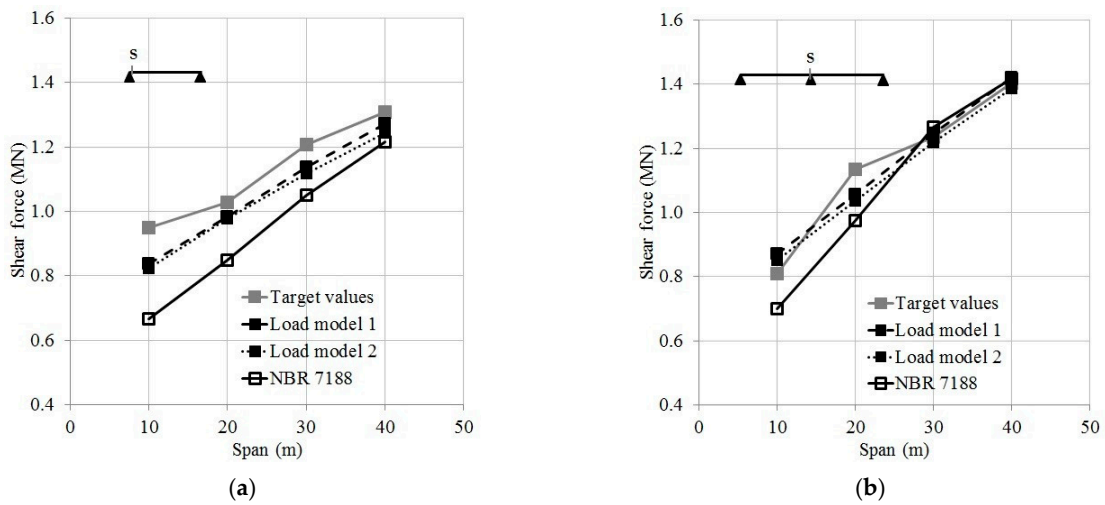


Figure 9. Comparison between the effects generated by the load models and the target values. (a) Shear forces on simply supported bridges. (b) Shear forces on continuous bridges.

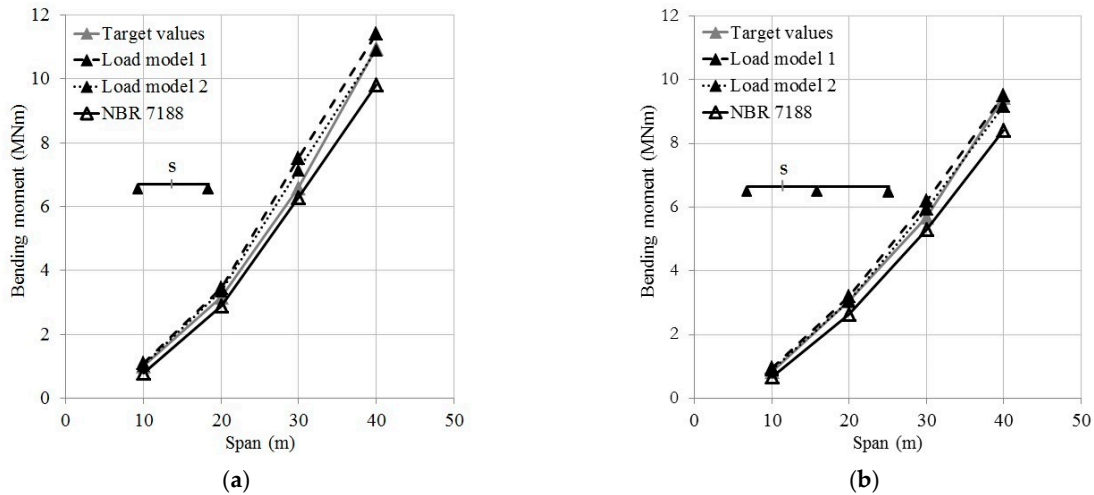


Figure 10. Comparison between the effects generated by the load models and the target values. (a) Positive moments on simply supported bridges. (b) Positive moments on continuous bridges.

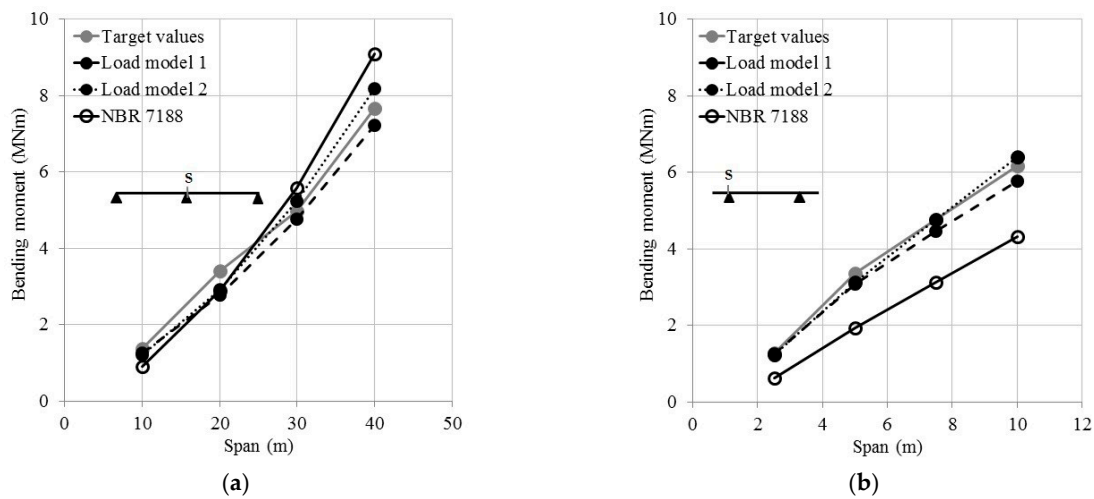


Figure 11. Comparison between the effects generated by the load models and the target values. (a) Negative moments on continuous bridges. (b) Negative moments on cantilevers.

Relative to the proposed load models 1 and 2, it can be seen that: (i) the negative moments were reasonably reproduced, except for the C-20 bridge; (ii) reasonable correlation was also achieved for the shear forces, except for the S-10 bridge; and (iii) the positive moments were the best represented effects by the new load models proposed.

For the NBR 7188 load model, the results show that in most cases (20 among 24), the current Brazilian design code underestimates the effects of the actual traffic, especially for the negative moments in cantilevers and the shear forces in shorter bridges; the only exception is the negative moment in the continuous bridges C-30 and C-40. It finally confirms the conclusions noted earlier [30,31], that the NBR 7188 standard does not properly represent the estimated extreme effects of the actual traffic and may need to be updated, as it appeared to be considerably against safety in some situations, whereas in others, it was considerably favorable to safety, which implies uneconomic design. The weighted error for the TB-450 model is 17.4%.

10. Conclusions

This paper presents and describes some of the steps performed to evaluate the current live load model of the Brazilian highway bridges design code and to develop new ones to adequately represent the extreme effects imposed by actual traffic. From the collection and acquisition of traffic data, the assembly of a database, and consideration of structural models in adjusted grids representing typical girder-type short span highway bridges, simulations of free-flow traffic were carried out to obtain static responses at critical cross-sections. Then, dynamic analyses were performed, considering the interaction between vehicles, bridges' structure, and pavement, aiming to obtain dynamic amplification factors representative of heavy traffic, which multiply the static characteristic values (determined by the extrapolation of the effects' PDF).

The main contributions and conclusions can be summarized as follows:

- (a) Two load models were proposed to represent the Brazilian commercial traffic. One of them considers a single design lane and the design vehicle located in the worst transverse position (as in NBR 7188 current model). The other one divides the effective deck width into three traffic lanes, which is the same configuration as the Eurocode 1 model LM1.
- (b) Neither the current NBR 7188 code load model (TB-450) nor the two proposed ones were able to fit traffic effects in all possible situations. Discrepancies between the target values and the effects caused by the proposed load models illustrate the difficulty in simultaneously fulfilling several requirements, a remarkable feature of multi-objective optimization problems.
- (c) However, the representativeness of the new proposed load models is considerably greater than the one from current NBR 7188 load model.
- (d) Results reiterate that TB-450 may not adequately represent the effects of the actual commercial traffic vehicles on the most representative bridges from the national highways network.

Next work steps compass:

- Inclusion of longer spans (in mixed flow and jams).
- Acquisition of more recent WIM traffic data.
- Recalibration of the load models.
- Calibration of load and resistance factors via structural reliability analyses.

Author Contributions: Conceptualization, C.E.R. and M.S.P.; methodology, C.E.R., M.S.P. and L.V.S.S.; software, C.E.R. and H.M.d.O.; formal analysis, C.E.R. and H.M.d.O.; investigation, C.E.R. and H.M.d.O.; writing—original draft preparation, C.E.R.; writing—review and editing, M.S.P.; supervision, M.S.P. and L.V.S.S.; funding acquisition, M.S.P. and L.V.S.S. All authors have read and agreed to the published version of the manuscript.

Funding: This research was financed in part by the Coordenação de Aperfeiçoamento de Pessoal de Nível Superior—Brasil (CAPES)—Finance Code 001. This research has also received funding from CNPq-Conselho Nacional de Desenvolvimento Científico e Tecnológico, Brazil.

Institutional Review Board Statement: Not applicable.

Informed Consent Statement: Not applicable.

Data Availability Statement: The data presented in this study are available on request from the corresponding author.

Conflicts of Interest: The authors declare no conflict of interest.

References

1. O'Brien, E.J.; Leahy, C.; Enright, B.; Caprani, C.C. Validation of Scenario Modelling for Bridge Loading. *Balt. J. Road Bridge Eng.* **2016**, *11*, 233–241. [[CrossRef](#)]
2. Enright, B.; O'Brien, E.J. Monte Carlo simulation of extreme traffic loading on short and medium span bridges. *Struct. Infrastruct. Eng.* **2013**, *9*, 1267–1282. [[CrossRef](#)]
3. Soriano, M.; Casas, J.R.; Ghosn, M. Simplified probabilistic model for maximum traffic load from weigh-in-motion data. *Struct. Infrastruct. Eng.* **2017**, *13*, 454–467. [[CrossRef](#)]
4. O'Connor, A.; O'Brien, E.J. Traffic load modelling and factors influencing the accuracy of predicted extremes. *Can. J. Civ. Eng.* **2005**, *32*, 270–278. [[CrossRef](#)]
5. Anitori, G.; Casas, J.R.; Ghosn, M. WIM-Based Live-Load Model for Advanced Analysis of Simply Supported Short- and Medium-Span Highway Bridges. *J. Bridge Eng.* **2017**, *22*, 04017062. [[CrossRef](#)]
6. O'Brien, E.J.; Schmidt, F.; Hajializadeh, D.; Zhou, X.-Y.; Enright, B.; Caprani, C.C.; Wilson, S.; Sheils, E. A review of probabilistic methods of assessment of load effects in bridges. *Struct. Saf.* **2015**, *53*, 44–56. [[CrossRef](#)]
7. O'Brien, E.J.; Caprani, C.C. Headway modelling for traffic load assessment of short to medium span bridges. *Struct. Eng.* **2005**, *83*, 33–36.
8. Bailey, S.F.; Bez, R. Site specific probability distribution of extreme traffic action effects. *Probabilistic Eng. Mech.* **1999**, *14*, 19–26. [[CrossRef](#)]
9. O'Brien, E.J.; Enright, B.; Getachew, A. Importance of the tail in truck weight modeling for bridge assessment. *J. Bridge Eng.* **2010**, *15*, 210–213. [[CrossRef](#)]
10. European Committee for Standardization. Eurocode 1: Basis of design and actions on structures. In *Part 1.2: Traffic Loads on Bridges*; European Committee for Standardization: Brussels, Belgium, 2005.
11. Calgaro, J.A. Loads on bridges. *Prog. Struct. Eng. Mater.* **1998**, *1*, 452–461. [[CrossRef](#)]
12. Babu, A.R.; Iatsko, O.; Nowak, A.S. Comparison of Bridge Live Loads in US and Europe. *Struct. Eng. Int.* **2019**, *29*, 84–93. [[CrossRef](#)]
13. Prat, M. Traffic load models for bridge design: Recent developments and research. *Prog. Struct. Eng. Mater.* **2001**, *3*, 326–334. [[CrossRef](#)]
14. American Association of State Highway and Transportation Officials. *AASHTO LRFD Bridge Design Specifications*; AASHTO: Washington, DC, USA, 2014.
15. Nowak, A.S. Live load model for highway bridges. *Struct. Saf.* **1993**, *13*, 53–66. [[CrossRef](#)]
16. Leahy, C.; O'Brien, E.J.; Hajializadeh, D. Review of HL-93 bridge traffic load model using an extensive database. *J. Bridge Eng.* **2015**, *20*, 04014115. [[CrossRef](#)]
17. Nowak, A.S. Calibration of LRFD Bridge Code. *J. Struct. Eng.* **1995**, *121*, 1245–1251. [[CrossRef](#)]
18. Iatsko, O.; Nowak, A.S. Revisited Live Load for Simple-Span Bridges. *J. Bridge Eng.* **2020**, *26*, 04020114. [[CrossRef](#)]
19. Miao, T.J.; Chan, T.H.T. Bridge live load models from WIM data. *Eng. Struct.* **2002**, *24*, 1071–1084. [[CrossRef](#)]
20. Heywood, R.; Gordon, R.; Bouilly, G. Australia's Bridge Design Load Model: Planning for an Efficient Road Transport Industry. *Transp. Res. Rec.* **2000**, *1696*, 1–7. [[CrossRef](#)]
21. Van Der Spuy, P.; Lenner, R. Towards a New Bridge Live Load Model for South Africa. *Structure* **2019**, *29*, 292–298. [[CrossRef](#)]
22. García-Soto, A.D.; Hernández-Martínez, A.; Valdés-Vázquez, J.G. Probabilistic assessment of a design truck model and live load factor from weigh-in-motion data for Mexican Highway bridge design. *Can. J. Civ. Eng.* **2015**, *42*, 970–974. [[CrossRef](#)]
23. *NBR7188*; Road and Pedestrian Live Load on Bridges, Viaducts, Footbridges and Other Structures. Brazilian Association of Technical Standards: Rio de Janeiro, Brazil, 2013.
24. Rossigali, C.E. Update in Live Load Model for Small-Span Highway Bridges in Brazil. Ph.D. Thesis, Federal University of Rio de Janeiro, Rio de Janeiro, Brazil, 2013. (In Portuguese)
25. Oliveira, H.O. Adjustment of the Live Load Model for Highway Bridges in Brazil. Master's Thesis, Federal University of Rio de Janeiro, Rio de Janeiro, Brazil, 2019. (In Portuguese)
26. Portela, E.L. Analysis and Development of a Live Load Model for Brazilian Concrete Bridges Based on WIM Data. Ph.D. Thesis, University of Sao Paulo, Sao Paulo, Brazil, 2018.

27. Mota, H.C. Extreme Effects on Bridges for Dynamic load Model in Brazil. Master's Thesis, Federal University of Rio de Janeiro, Rio de Janeiro, Brazil, 2017. (In Portuguese)
28. Carneiro, A.L.; Portela, E.L.; Bittencourt, T.N. Development of Brazilian highway live load model for unlimited fatigue life. *IBRACON Struct. Mater. J.* **2020**, *13*, e13407. [[CrossRef](#)]
29. Ghosn, M.; Moses, F. Reliability calibration of bridge design code. *J. Struct. Eng.* **1986**, *112*, 745–763. [[CrossRef](#)]
30. Rossigali, C.E.; Pfeil, M.S.; Battista, R.C.; Sagrilo, L.V.S. Towards actual Brazilian traffic load models for short span highway bridges. *Ibracon Struct. Mater. J.* **2015**, *8*, 124–139. [[CrossRef](#)]
31. Rossigali, C.E.; Pfeil, M.S.; Sagrilo, L.V.S. Update in values of traffic effects on Brazilian short span bridges. In Proceedings of the International Conference on Bridge Maintenance, Safety and Management, Foz do Iguaçu, Brazil, 26–30 June 2016.
32. Portela, E.L.; Teixeira, R.M.; Bittencourt, T.N.; Nassif, H. Single and multiple presence statistics for bridge live load based on weigh-in-motion data. *Ibracon Struct. Mater. J.* **2017**, *10*, 1163–1173. [[CrossRef](#)]
33. Liu, Y.; Zhang, H.; Deng, Y.; Jiang, N. Effect of live load on simply supported bridges under a random traffic flow based on weigh-in-motion data. *Adv. Struct. Eng.* **2017**, *20*, 722–736. [[CrossRef](#)]
34. NBR6118; Design of Concrete Structures–Procedure. Brazilian Association of Technical Standards: Rio de Janeiro, Brazil, 2014.
35. Santos, C.A.N.; Battista, R.C.; Pfeil, M.S. Retro analysis of an urban bridge through theoretical-numerical-experimental technique, In Proceedings of the EVACES'13, Ouro Preto, Brazil, 28–30 October 2013.
36. Miluccio, G.; Losanno, D.; Parisi, F.; Cosenza, E. Fragility analysis of existing prestressed concrete bridges under traffic loads according to new Italian guidelines. *Struct. Concr.* **2022**, *6*, 1–17. [[CrossRef](#)]
37. Stucchi, F.R.; Luchi, L.A.R. Real road load compared to standard load for Brazilian bridges. *Proc. ICE-Bridge Eng.* **2015**, *168*, 245–258. [[CrossRef](#)]
38. O'Brien, E.J.; Enright, B. Using weigh-in-motion data to determine aggressiveness of traffic for bridge loading. *J. Bridge Eng.* **2013**, *18*, 232–239. [[CrossRef](#)]
39. Das, P.C. *Safety of Bridges*; Thomas Telford: London, UK, 1997.
40. O'Brien, E.J.; Enright, B. Modeling same-direction two-lane traffic for bridge loading. *Struct. Saf.* **2011**, *33*, 296–304. [[CrossRef](#)]
41. Nowak, A.S.; Nassif, H.; DeFrain, L. Effect of truck loads on bridges. *J. Transp. Eng.* **1993**, *119*, 853–867. [[CrossRef](#)]
42. Frýba, L. *Vibration of Solids and Structures under Moving Loads*; Thomas Telford: London, UK, 1972.
43. Cebon, D. *Handbook of Vehicle-Road Interaction*; Sewts & Zeitlinger: Lisse, The Netherlands, 1999.
44. Kim, C.W.; Kawatani, M.; Kim, K.B. Three-dimensional dynamic analysis for bridge-vehicle interaction with roadway roughness. *Comput. Struct.* **2005**, *83*, 1627–1645. [[CrossRef](#)]
45. Battista, R.C.; Pfeil, M.S. Bridge dynamics and aerodynamics: Design and practical requirements for high structural performance and safety. *Struct. Infrastruct. Eng.* **2018**, *14*, 491–508. [[CrossRef](#)]
46. De Risi, R. A computational framework for finite element modeling of traveling loads on bridges in dynamic regime. *Comput. Aided Civ. Inf.* **2022**, *37*, 470–484. [[CrossRef](#)]
47. Honda, H.; Kajikawa, Y.; Kobori, T. Spectra of Road Surface Roughness on Bridges. *J. Struct. Div. ASCE* **1982**, *108*, 1956–1966. [[CrossRef](#)]
48. Ludescher, H.; Brühwiler, E. Dynamic Amplification of Traffic Loads on Road Bridges. *Struct. Eng. Int.* **2009**, *19*, 190–197. [[CrossRef](#)]
49. Brady, S.P.; O'Brien, E.J.; Žnidarič, A. The effect of vehicle velocity on the dynamic amplification of a vehicle crossing a simply supported bridge. *J. Bridge Eng.* **2006**, *11*, 241–249. [[CrossRef](#)]
50. Pfeil, M.S.; Rossigali, C.E.; Battista, R.C.; Mendonça, R.F. Live load model proposal for Brazilian highway bridges of small spans. In Proceedings of the XXXIV South American Journeys on Structural Engineering, San Juan, Argentina, 27 September–1 October 2010.
51. Cantero, D.; Gonzáles, A.; O'Brien, E.J. Comparison of Bridge Dynamic Amplifications due to Articulated 5-Axle Trucks and Large Cranes. *Balt. J. Road Bridge Eng.* **2011**, *6*, 39–47. [[CrossRef](#)]

Disclaimer/Publisher's Note: The statements, opinions and data contained in all publications are solely those of the individual author(s) and contributor(s) and not of MDPI and/or the editor(s). MDPI and/or the editor(s) disclaim responsibility for any injury to people or property resulting from any ideas, methods, instructions or products referred to in the content.